# Design of Ductile Rare-Earth-Free Magnesium Alloys

W. A. Curtin, Rasool Ahmad, Binglun Yin, and Zhaoxuan Wu

**Abstract**

Pure Mg has low ductility due to a transition of $\langle c+a \rangle$ pyramidal dislocations to a sessile basal-oriented structure. Dilute alloying generally improves ductility. Enhancement of pyramidal cross-slip from the lower-energy pyramidal II plane to the higher-energy pyramidal I plane has been proposed as the mechanism. Here, the theory is applied to ternary and quaternary alloys of Zn, Al, Li, Ca, Mn, Sn, K, Zr, and Sr at dilute concentrations, and a wide range of compositions are predicted to have good ductility. Interestingly, while Zn alone is insufficient for achieving ductility, its inclusion in multicomponent alloys at 0.5 at.% enables ductility at the lowest concentrations of other alloying elements. Further implications of the theory are discussed.

**Keywords**

Magnesium alloys • Theory • Ductility

## Introduction

Magnesium (Mg) is the lightest structural metal but has a hexagonal close packed (HCP) crystal structure. The HCP structure has crystallographically different slip systems with distinct slip planes (basal, prism, and pyramidal), slip steps ($\langle a \rangle$ and $\langle c+a \rangle$ Burgers vectors) and slip resistance ($\gamma$-surface). Generally, plastic slip with $\langle a \rangle$ dislocations on basal and prism planes is intrinsically easier than that of $\langle c+a \rangle$ dislocations on pyramidal planes, as dictated by crystallography and the electronic structure of Mg in the HCP lattice [1]. Furthermore, $\langle c+a \rangle$ dislocations dissociated on pyramidal glide planes are thermodynamically unstable and can transform into lower energy, sessile structures along basal planes through pyramidal-to-basal (PB) transition [2]. The energy barriers of the $\langle c+a \rangle$ PB transitions are low ($\sim$0.5 eV for pyramidal II plane [2] and $\sim$0.3 eV for pyramidal I plane [3]) and comparable to other plasticity mechanisms at room temperature. Plastic slip with $\langle c+a \rangle$ dislocations can thus only provide very limited $\langle c \rangle$ axis strain capability initially upon their activation; the PB transition will quickly increase the critical resolved shear stress (CRSS) for $\langle c+a \rangle$ slip systems and effectively eliminate the critical $\langle c+a \rangle$ dislocation slip systems [2]. The PB transition thus further increases plastic anisotropy, with $\langle c+a \rangle$ CRSS measured at $\sim$100 times that of basal $\langle a \rangle$ [4]. The difficulty in $\langle c+a \rangle$ dislocation slip also contributes to strong textures developed in wrought Mg products, such as strong basal textures with $c$-axis in the normal direction of rolled sheets and strong fiber textures with $c$-axis in radial direction in extruded products. Strong plastic anisotropy and texture cause HCP Mg exhibit low ductility [2] and intrinsic brittleness [5], which are detrimental in load-carrying or energy-absorption structure applications.

Achieving high ductility and high fracture toughness in Mg is thus a long-standing barrier for its wide range, large-scale structure applications across various industries, such as the automotive and aerospace industries [6, 7]. Increasing ductility is, however, particularly challenging in HCP Mg, since its plastic anisotropy arises from the intrinsic properties of the slip systems and changing intrinsic properties is difficult. Increasing ductility is also generally less straightforward as compared to increasing strength, since the former depends on the plastic evolution of the underlying microstructure. Various metallurgical strategies, such as

W. A. Curtin (✉) · R. Ahmad · B. Yin
Laboratory for Multiscale Mechanics Modeling, Institute of Mechanical Engineering, EPFL, 1015 Lausanne, Switzerland
e-mail: william.curtin@epfl.ch

R. Ahmad
e-mail: rasool.ahmad@epfl.ch

B. Yin
e-mail: binglun.yin@epfl.ch

Z. Wu
Department of Materials Science and Engineering, City University of Hong Kong, Tat Chee Avenue, Kowloon, Hong Kong, China
e-mail: zhaoxuwu@cityu.edu.hk

© The Minerals, Metals & Materials Society 2020
J. B. Jordon et al. (eds.), *Magnesium Technology 2020*, The Minerals, Metals & Materials Series, https://doi.org/10.1007/978-3-030-36647-6_5

changing alloy composition, grain size, and texture, have been attempted to increase ductility and fracture toughness. Improved ductility has been demonstrated in some Mg alloys and under certain thermomechanical processing conditions. In particular, a wide range of experimental studies suggest that Mg alloyed with rare-earth elements in solid solution state [8–13], grain refinement [14] and texture randomization [15, 16] are effective methods to increase ductility. While these experimental successes are consistent with metallurgical wisdom, current understanding of ductility improvement in Mg is generally empirical, not mechanistic, qualitative, and thus of less predictive power in guiding new alloy designs.

We recently proposed a new quantitative mechanism [14] to capture the effects of solutes in enhancing ductility in Mg alloys. This mechanism is based on the acceleration of cross-slip of the pyramidal II $\langle \boldsymbol{c}+\boldsymbol{a} \rangle$ screw dislocations due to a solute-driven decrease in the cross-slip energy barrier. If the acceleration is significant enough, cross-slip will enable fast $\langle \boldsymbol{c}+\boldsymbol{a} \rangle$ dislocation multiplication that can generate plastic strain in spite of the on-going deleterious PB transitions (Fig. 1). The predictions based on the new mechanistic model were shown to be in broad agreement with experimental results on existing Mg alloys. Moreover, application of the mechanistic model to study a much wider range of possible alloys, especially those without RE additions, holds the promise of accelerating the design of new ductile Mg.

In this work, we briefly present key features of the model for solute-enhanced cross-slip and then focus on the predictions of the model for a range of non-RE multicomponent alloys. This work summarizes a much more complete study that was recently published by the same authors [17], and many details can be found there.

## Ductility Enhancement via Accelerated Cross-Slip: Theory

Plastic slip via $\langle \boldsymbol{c}+\boldsymbol{a} \rangle$ dislocations are critical to achieving high ductility in HCP Mg. During plastic straining, $\langle \boldsymbol{c}+\boldsymbol{a} \rangle$ dislocation loops, either preexisting inside grains or nucleated from grain boundaries, will expand and carry the plastic strain. The edge segments of the dislocation loop are prone to undergo the PB transition and become sessile, locking the dislocation segments and further blocking subsequent $\langle \boldsymbol{c}+\boldsymbol{a} \rangle$ dislocations on the same or nearby parallel pyramidal planes. Plastic slip in the $\langle \boldsymbol{c}+\boldsymbol{a} \rangle$ dislocation Burgers vector direction thus becomes difficult, requiring a much higher CRSS to continue [2]. While the edge segments become sessile, the screw segments can continue to glide, expand,

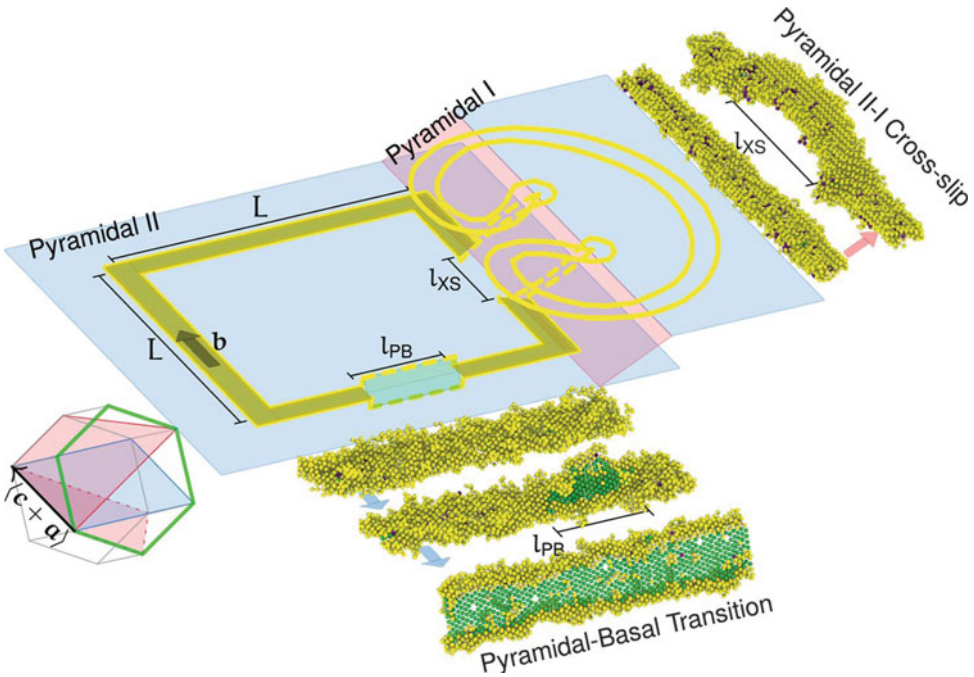


**Fig. 1** Schematic of the competing thermally activated dislocation phenomena in magnesium. Mobile edge dislocation segments of a pyramidal II $\langle \boldsymbol{c}+\boldsymbol{a} \rangle$ dislocation undergo a thermally activated transformation to a sessile structure with a barrier of $\Delta G_{PB} = 0.5$eV. Mobile screw dislocation segments of the same dislocation can undergo thermally activated cross-slip and double cross-slip, leading to dislocation multiplication, with a barrier of $\Delta G_{XS}$. If the rate of screw cross-slip sufficiently exceeds the rate of edge immobilization, then plastic straining can be sustained and high ductility can be achieved. Solute additions can change the cross-slip barrier $\Delta G_{XS}$ which, if reduced sufficiently by solutes, can provide the conditions for ductility. From Ref. [14], and reprinted with permission from AAAS

and potentially undergo a cross-slip and double cross-slip process. Dislocation cross-slip and double cross-slip effectively create a new dislocation loop on a new slip plane, which can overcome the locking of the original edge segment, and glide further to accommodate the imposed plastic strain. The newly formed dislocation loop can also serve as a $\langle \boldsymbol{c}+\boldsymbol{a} \rangle$ dislocation Frank–Read source, potentially supplying many new $\langle \boldsymbol{c}+\boldsymbol{a} \rangle$ dislocations. To sustain plastic slip along the $\langle \boldsymbol{c}+\boldsymbol{a} \rangle$ direction and thus satisfying strain compatibility requirement for continued plastic deformation, the rate of cross-slip of the screw segments and thus generation of new dislocation loops must be much faster than the rate of the deleterious PB transition occurring at the edge segments. The two crucial processes at the screw and edge segments are both thermally activated and their competition governs the $\langle \boldsymbol{c}+\boldsymbol{a} \rangle$ strain capability and ductility. To achieve high ductility, the following condition on their respective rates $R_{XS}$ and $R_{\mathrm{PB}}$ along the dislocation loop of size $L$ occurring at segments of size $l_{XS}$ and $l_{\mathrm{PB}}$ (see Fig. 1) at temperature $T$ must be satisfied,

$$R_{XS} = \nu_0 \frac{L}{l_{XS}} \exp\left(-\frac{\Delta G_{XS}}{kT}\right) \gg R_{\mathrm{PB}} = \nu_0 \frac{L}{l_{\mathrm{PB}}} \exp\left(-\frac{\Delta G_{\mathrm{PB}}}{kT}\right) \tag{1}$$

where $G_{XS}$ and $G_{\mathrm{PB}}$ are the activation energy barriers, $\nu_0$ is an attempt frequency and $k$ is Boltzmann constant. We introduce a ductility index $\chi$ where the rate of cross-slip is $10^{\chi}$ of the rate of PB transition, i.e., $R_{XS} = 10^{\chi} R_{\mathrm{PB}}$. We consider $\chi > 1$, i.e., $R_{XS} > 10R_{\mathrm{PB}}$, as a necessary condition for high ductility. For alloys satisfying the above condition, deformation will follow normal plastic flow and hardening, and failure may be governed by other criteria such as the Consider criterion for the onset of necking in elastic-plastic materials. When $\chi < 0$, poor ductility is predicted since $\langle \boldsymbol{c}+\boldsymbol{a} \rangle$ cross-slip is too slow relative to the PB transition and cannot create enough $\langle \boldsymbol{c}+\boldsymbol{a} \rangle$ dislocation and plastic strain to overcome the immobilization caused by the PB transition. Our strategy to enhance ductility relies mainly on reducing the cross-slip barrier $\Delta G_{XS}$ through solid solution alloying, since all other parameters are insensitive to changes of alloy compositions. Solutes interact with dislocation core, stacking fault and its elastic field. Solutes can thus have subtle effects on dislocation cross-slip energy barriers and rates [18]. The central part of the theory and alloy design thus essentially reduce to the determination of the effects of solutes on the cross-slip barrier $\Delta G_{XS}$ as a function of solute composition and concentration.

In HCP structures, pyramidal II planes do not intersect with each other and $\langle \boldsymbol{c}+\boldsymbol{a} \rangle$ dislocations on pyramidal II planes must first cross-slip to an intersecting pyramidal I plane sharing the same Burgers vector. In HCP Mg, screw $\langle \boldsymbol{c}+\boldsymbol{a} \rangle$ dislocations have lower energy on pyramidal II planes than on pyramidal I planes. The energy barrier for cross-slip thus has contributions from the dislocation energy difference $\Delta E^{\mathrm{I-II}}$ between the two pyramidal planes, in addition to the usual energies associated with dislocation jog/junctions formations and line tensions. Using the dislocation line tension model, the cross-slip energy barrier can be written as

$$\Delta G_{XS} = \Delta G_{XS,i} + \Delta E^{\mathrm{I-II}} l_{XS} + \Gamma \Delta s(l_{CXS}) - \Delta\tau b A(l_{CXS}) \tag{2}$$

where $\Delta G_{XS,i} = 0.23\,\mathrm{eV}$ [19] is the intrinsic barrier associated with jog/junctions formation during cross-slip; $l_{XS}$ is the length of the cross-slip nucleus at the transition state, $l_{CXS}$ the nucleation length that includes the length of the pyramidal I/II junction, $\Gamma$ is the screw dislocation line tension on pyramidal I planes, $b$ the Burgers vector, $\Delta s$ the additional length of the cross-slipped bow-out segment on the pyramidal I plane, $A$ the bow-out area, and $\Delta\tau$ the resolved shear stress on the pyramidal I $\langle \boldsymbol{c}+\boldsymbol{a} \rangle$ dislocation in excess of the corresponding CRSS that performs work by bowing out the cross-slipping nucleus.

A solute at site $i$ can interact with the dislocation on the pyramidal II plane before cross-slip and with the dislocation on the pyramidal I plane after cross-slip. The change in interaction energy of a solute of type $m$ at site $i$ is denoted as $\Delta U_i^{\mathrm{I-II},m}$. The average change in energy per unit dislocation length upon cross-slip can then be written as

$$\langle \Delta E^{\mathrm{I-II}} \rangle = \Delta E_{\mathrm{Mg}}^{\mathrm{I-II}} + \frac{1}{b} \sum_m c_m \sum_{i \in N_T} \Delta U_i^{\mathrm{I-II},m} \tag{3}$$

where $\Delta E_{\mathrm{Mg}}^{\mathrm{I-II}}$ is the energy difference in pure Mg, $c_m$ is the solute concentration of solute type $m$, and the sum is over all unique sites $i$ around the dislocation within one Burgers vector length where the energy difference is nonzero. These energies cannot be computed fully with ease, and hence, it was postulated that the dominant interaction energy arises from the solute interactions with the dislocation stacking faults, as both pyramidal I and II dislocations are dissociated into partial dislocations separated by a stacking fault. The average energy difference can then expressed as

$$\langle \Delta E^{\mathrm{I-II}} \rangle = \Delta E_{\mathrm{Mg}}^{\mathrm{I-II}} + \sum_m \Delta E_{\mathrm{avg,SF}}^{\mathrm{I-II},m} c_m \tag{4}$$

where $\Delta E_{\mathrm{avg,SF}}^{\mathrm{I-II},m}$ is the contribution of type $m$ solute/stacking fault interaction energies in the average dislocation energy difference. $\Delta E_{\mathrm{avg,SF}}^{\mathrm{I-II},m}$ is computed from first-principles density functional theory calculations [1, 17]. In a random solid solution alloy, there are local fluctuations in the concentration of the alloying elements. Thus, there are fluctuations in the local pyramidal I and II screw dislocation energies over

the scale of the nucleation length $l_{XS}$. The standard deviation in pyramidal I/II energy difference, due to these fluctuations, over the length of $l_{XS}$ can be computed as

$$\sigma[l_{XS}] = \sqrt{\frac{l_{XS}}{b}\sum_m c_m \sum_{i\in N_T}\left(\Delta U_i^{\mathrm{I-II},m}\right)^2} = \sqrt{\frac{l_{XS}}{b}\sum_m c_m \left(\Delta E_{\mathrm{fluc,SF}}^{\mathrm{I-II},m}\right)^2} \quad (5)$$

where the second term considers only the energy contributions due to the solute/stacking fault interactions. Some fluctuations raise the energy and others lower it; only those that reduce the local barrier are relevant, and so the magnitude of the fluctuation contribution is always subtracted from the average barrier to obtain the operative barrier. Assembling all the factors that determine the activation barrier and critical cross-slip nucleation length, the ductility index $\chi$ can be expressed as

$$\chi = \frac{1}{\ln 10}\left[\ln\left(\frac{l_{\mathrm{PB}}}{l_{XS}}\right) + \frac{\Delta G_{\mathrm{PB}} - (\langle \Delta G_{XS}\rangle - \sigma[l_{XS}])}{kT}\right]. \quad (6)$$

The DFT calculations on a wide range of solutes led to the determination of the average and fluctuation contributions to the energy barrier as shown in Fig. 2. Figure 2 immediately shows that the rare-earth elements and Zr are highly effective in reducing the cross-slip barrier, both on average and due to fluctuations. The solutes Ca and Sr are also effective on average, being negative, with significant fluctuations as well, while Mn is effective on average but with smaller fluctuation contributions. The solutes Sn, Li, and K have almost no effect on average, but some fluctuation contribution, especially K. The solutes Zn, Al, and Ag are all, on average, deleterious for ductility, but the fluctuation contributions, being always negative, can cancel or exceed the average contributions at some concentrations, leading to some reduction of the ductility index $\chi$.

More detailed predictions of $\chi$ require the full theory. Two quantities that are not directly computable in the theory, but fall in a narrow range and can be estimated, are $\Delta E_{\mathrm{Mg}}^{\mathrm{I-II}}$ and $\Delta\tau$. Examination of theory predictions versus experiments for the well-established solute elements of Al, Zn, and Y led to the deduction of $\Delta E_{\mathrm{Mg}}^{\mathrm{I-II}} = 25$ meV/nm and $\Delta\tau = 20$ MPa. Finally, for very low solute concentrations, where single solutes may have some effect and random statistics does not apply, additional analysis is required (see Ref. [17]).

## Representative Results

We now present a subset of results on ternary and quaternary alloys. The theory is used to compute $\chi$ as a function of alloy composition, and ductility is indicated if $\chi > 1$. Since Zn is a common alloying element for various reasons, we first consider Zn ternary alloys. Zn alone is not predicted to enable ductility—the negative fluctuation contribution is never large enough compared to the positive average contribution to reduce $\chi$ below 0. However, since Zn does lower $\chi$ relative to pure Mg, it has a beneficial effect when combined with other more favorable solutes. Figure 3a shows the predictions for $\chi$ as a function of the Zn concentration and the concentration of a third alloy element X (X=K, Mn, Zr, Sr, Ca). In all cases, Mg can be made ductile by the addition of a small concentration of X as long as the concentration of Zn is less than about 1.5 at.%. For all cases, the addition of 0.5 at.% Zn enables ductility at the lowest concentration of the second element X. The effect is especially strong for Mn, where $\chi = 1$ is reduced from ~0.4 at.% Mn at 0 at.% Zn to ~0.2 at.% Mn at 0.5 at.% Zn. The theory thus predicts that the addition of Zn at 0.5 at.% is broadly useful for enhancing the ductility across a range of alloys. Zn is not necessary for ductility, but its addition may be beneficial for other reasons such as its effects on the $\langle a\rangle$ dislocations.

Figure 3b shows predictions for the ductility limit $\chi = 1$ for various Al–Li–X quaternary alloys, for X=Mn, K, Sr. The lines in the figure correspond to the boundary between

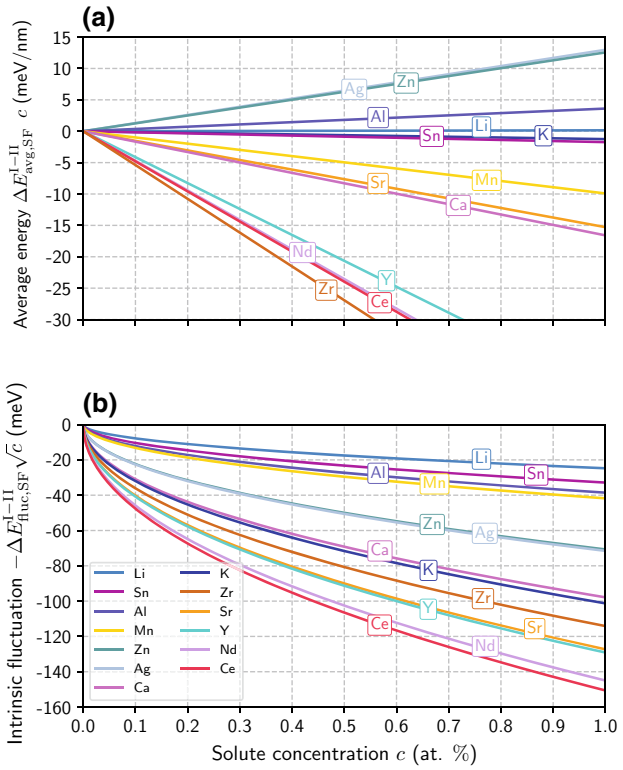


**Fig. 2** Variation of (**a**) average effect and (**b**) intrinsic fluctuation of various solutes on pyramidal I/II $\langle \boldsymbol{c}+\boldsymbol{a}\rangle$ dislocation energy difference as a function of corresponding solute concentrations $c$. From Ref. [17], and reprinted with permission from Elsevier

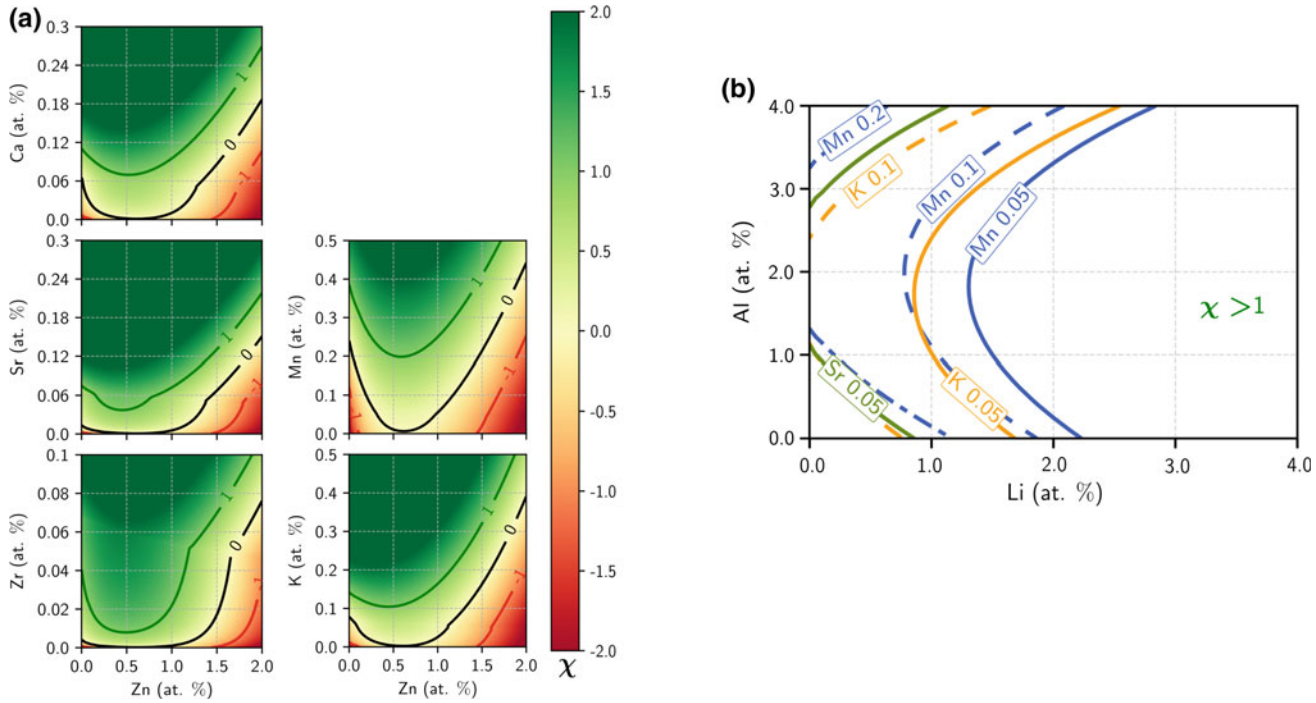


**Fig. 3** **a** Ductility index $\chi$ for a range of Mg–Zn–X ternary alloys. $\chi > 1$ corresponds to predictions of good ductility, while $\chi < 0$ corresponds to predictions of poor ductility. A wide range of composition space, at very low alloying concentrations, is predicted to enable ductility in these ternary alloys. **b** Ductility index $\chi$ for a range of Mg–Al–Li quaternary alloys. $\chi > 1$ corresponds to predictions of good ductility, while $\chi < 0$ corresponds to predictions of poor ductility. A wide range of composition space, at very low alloying concentrations, is predicted to enable ductility in these quaternary alloys. Adapted from Ref. [17], and reprinted with permission from Elsevier

$\chi > 1$ (right) and $\chi < 1$ (left), for each concentration of X indicated. For instance, in the Mg–Al–Li–Mn quaternary, ductility ($\chi > 1$) can be achieved at 2.0 at.% Al, 1.0 at.% Li with the addition of 0.1 at.% Mn. Many other examples are provided in similar graphical form in the related publication [17].

## Discussion

The theory makes predictions for a wide range of alloying elements and compositions that can lead to high ductility. This wide space thus enables possible optimization of other important alloy properties (e.g. yield strength, toughness, corrosion resistance, and bio-compatibility) that are needed for using Mg alloys in various applications. Related to strengthening, we note that precipitation removes solutes from the matrix. If the residual total solute concentrations in the matrix are too low, the matrix composition may drop below the conditions predicted for ductility. The strengthening that accompanies precipitation may then lead to a significant reduction in ductility. The identification here of a wide range of ductilizing alloying elements at low concentrations opens, however, the possibility that alloys can be developed with elements that form desirable precipitates and other elements that remain in solution such that the matrix remains ductile after precipitation, thus achieving both strength and ductility. Pursuing such concepts requires combining the present analysis of ductility with thermodynamic calculations of phase diagrams and solution limits of alloying elements in complex alloys.

**Acknowledgements** WAC and RA acknowledge financial support of this work through a grant from the Swiss National Science Foundation entitled "Control of Atomistic Mechanisms of Flow in Magnesium Alloys to Achieve High Ductility" (project #162350). The authors also acknowledge support from EPFL to the Laboratory for Multiscale Mechanics Modeling that enabled the required high-performance computing provided by Scientific IT and Application Support (SCITAS) at EPFL.

## References

1. B. Yin, Z. Wu, W. A. Curtin, Comprehensive first-principles study of stable stacking faults in hcp metals, Acta Materialia 123 (2017) 223–234.
2. Z. Wu, W. A. Curtin, The origins of high hardening and low ductility in magnesium, Nature 526 (2015) 62–67.
3. Z. Wu, W. A. Curtin, Intrinsic structural transitions of the pyramidal I $\langle c+a \rangle$ dislocation in magnesium, Scripta Materialia 116 (2016) 104–107.

4. H. Tonda, S. Ando, Effect of temperature and shear direction on yield stress by $\{11\bar{2}2\}\langle\bar{1}\bar{1}23\rangle$ slip in HCP metals, Metallurgical and Materials Transactions A 33 (2002) 831–836.
5. Z. Wu, W. A. Curtin, Brittle and ductile crack-tip behavior in magnesium, Acta Materialia 88 (2015) 1–12.
6. H. Friedrich, S. Schumann, Research for a "new age of magnesium" in the automotive industry, Journal of Materials Processing Technology 117 (2001) 276–281.
7. M. K. Kulekci, Magnesium and its alloys applications in automotive industry, International Journal of Advanced Manufacturing Technology 39 (2008) 851–865.
8. S. R. Agnew, J. W. Senn, J. A. Horton, Mg sheet metal forming: Lessons learned from deep drawing Li and Y solid-solution alloys, JOM 58 (2006) 62–69.
9. S. Sandlöbes, S. Zaefferer, I. Schestakow, S. Yi, R. Gonzalez-Martinez, On the role of non-basal deformation mechanisms for the ductility of Mg and Mg–Y alloys, Acta Materialia 59 (2011) 429–439.
10. S. Sandlöbes, M. Friák, J. Neugebauer, D. Raabe, Basal and non-basal dislocation slip in Mg–Y, Materials Science and Engineering: A 576 (2013) 61–68.
11. S. Sandlöbes, Z. Pei, M. Friák, L. F. Zhu, F. Wang, S. Zaefferer, D. Raabe, J. Neugebauer, Ductility improvement of Mg alloys by solid solution: Ab initio modeling, synthesis and mechanical properties, Acta Materialia 70 (2014) 92–104.
12. Y. Huang, W. Gan, K. U. Kainer, N. Hort, Role of multi-microalloying by rare earth elements in ductilization of magnesium alloys, Journal of Magnesium and Alloys 2 (2014) 1–7.
13. H. Rikihisa, T. Mori, M. Tsushida, H. Kitahara, S. Ando, Influence of yttrium addition on plastic deformation of magnesium, Materials Transactions 58 (2017) 1656–1663.
14. Z. Wu, R. Ahmad, B. Yin, S. Sandlöbes, W. A. Curtin, Mechanistic origin and prediction of enhanced ductility in magnesium alloys, Science 359 (2018) 447–452.
15. R. K. Mishra, A. K. Gupta, P. R. Rao, A. K. Sachdev, A. M. Kumar, A. A. Luo, Influence of cerium on the texture and ductility of magnesium extrusions, Scripta Materialia 59 (2008) 562–565.
16. R. K. Sabat, A. P. Brahme, R. K. Mishra, K. Inal, S. Suwas, Ductility enhancement in Mg-0.2% Ce alloys, Acta Materialia 161 (2018) 246–257.
17. R. Ahmad, B. Yin, Z. Wu, W. Curtin, Designing high ductility in magnesium alloys, Acta Materialia 172 (2019) 161–184.
18. W. G. Nöhring, W. A. Curtin, Dislocation cross-slip in fcc solid solution alloys, Acta Materialia 128 (2017) 135–148.
19. Z. Wu, W. A. Curtin, Mechanism and energetics of $\langle c+a\rangle$ dislocation cross-slip in hcp metals, Proceedings of the National Academy of Sciences 113 (2016) 11137–11142.